Section 3.5

Statistical Properties: Astrophysical Relationships

3.5. Statistical Properties: Astrophysical Relationships

In this section a number of astrophysical relationships in the Hipparcos Catalogue are illustrated. Most prominent of these are a set of Hertzsprung-Russell diagrams using two different systems of colour/magnitude representation, and for different selections of stars, based on their precision or other properties.

3.5.1. Hertzsprung-Russell Diagrams

Hertzsprung-Russell (HR) diagrams are presented in the form of (observational) luminosity-colour diagrams, with two choices for the photometric parameters: (i) M_V versus $B-V$, and (ii) M_{Hp} versus $V-I$. For a definition of these quantities, refer to Section 1.3. The absolute luminosities were computed as:

$$M_V = V + 5\log\pi - 10$$
$$M_{Hp} = Hp + 5\log\pi - 10$$

where the parallax, π, is in milliarcsec. Interpretation of the detailed astrophysical features of the observational HR diagram must take into account effects such as the *a priori* selection of stars in the catalogue, Lutz-Kelker bias (T.E. Lutz, D.H. Kelker, 1973, *Mon. Not. R. Astron. Soc.* 85, 573), and the fact that the expectation of the stellar distance can differ from that of the inverse of the parallax (H. Smith, H. Eichhorn, 1996, *Mon. Not. R. Astron. Soc.* 281, 211), effects which are ignored in the presentation of the observational properties of the catalogue in this section.

For the general HR diagrams three different sets of stars were selected according to the precision of their parallax and colour index:

(i) $\sigma_\pi/\pi < 0.05$ (corresponding to an error in the absolute magnitudes σ_M of about 0.1 mag), and standard error of the colour index $\sigma_{\rm CI} \le 0.025$;

(ii) $\sigma_\pi/\pi < 0.1$ (corresponding to $\sigma_M \simeq 0.2$ mag), and $\sigma_{\rm CI} \le 0.025$;

(iii) $\sigma_\pi/\pi < 0.2$ (corresponding to $\sigma_M \simeq 0.4$ mag), and $\sigma_{\rm CI} \le 0.05$.

where the subscript CI refers to the colour index ($B - V$ or $V - I$, as appropriate). Double stars have been excluded from most diagrams, as indicated in the captions. In the Hipparcos main catalogue, Hp magnitudes are often given for such systems for a combination of components (as indicated in Field H48, or in the Notes). Use of these magnitudes leads to a systematic over-estimation of the absolute magnitudes compared with those of single stars. For the diagrams where the caption indicates the inclusion of single stars only, catalogue entries included in any of the parts of the Double and Multiple Star Annex have been excluded.

Since the global Hipparcos Catalogue is not a complete catalogue in any sense, caution must be exercised in drawing conclusions of a statistical nature from the present diagrams; in general there will be a strong bias towards stars with a higher apparent

luminosity (cf. Figure 1.1.1), in particular for stars with less precisely determined distances (since the relative parallax precision is correlated with the parallax, cf. Figure 3.5.19).

Some of the most prominent features of the Hipparcos HR diagram have been discussed, for a preliminary version of the catalogue, by M.A.C. Perryman *et al.*, 1995, *Astron. Astrophys.* 304, 69.

Figures 3.5.1, 3.5.3, and 3.5.5 give $M_V, B-V$ diagrams for the three star selections. In these, and most of the following diagrams, the number of stars in a cell of size 0.01 mag in $B-V$ and 0.05 mag in M_V has been colour coded according to the (logarithmic) scale given in the figure. Figures 3.5.2, 3.5.4, and 3.5.6 give $M_{Hp}, V-I$ diagrams for the same three star selections.

Figure 3.5.7 illustrates the relative contributions from stars of the three precision classes to the diagram in Figure 3.5.6: i.e. the stars in set (i), the stars in set (ii) not occurring in (i), and the stars in set (iii) not in sets (i) and (ii). The lower end of the HR diagram, largely populated by nearby stars with well-determined distances, is dominated by stars in the highest precision class. The presence of a distinct 'spine' shows that the broadening of the diagram when including less precise data is not only due to the statistical effect of including more stars, but is also a consequence of the progressively degrading measurement accuracy. In general the 'wings' are mostly extended towards the brighter stars, a consequence of the selection effects intrinsic in the Hipparcos Catalogue.

Figure 3.5.8 illustrates that the fraction of stars that have a non-blank coarse variability flag (Field H6) is quite variable over the Hertzsprung-Russell diagram. Figures 3.5.9 and 3.5.10 give the position in the $M_{Hp}, V-I$ diagram for single and double stars with the coarse variability indicator (Field H6) set. Almost all very red giants are variable in the category 2 (i.e. variability amplitude in the range 0.06–0.6 mag). Stars with variability amplitude larger than 0.6 mag are almost all on the main sequence. Mira variables could be expected to appear on the giant branch; only one such variable in the Hipparcos Catalogue meets both criteria on precision, however.

The subsequent diagrams show the position of stars of different variability categories in the $M_{Hp}, V-I$ diagram: eclipsing binaries in Figure 3.5.11; pulsating variables in Figure 3.5.12; rotating variables in Figure 3.5.13; and eruptive variables in Figure 3.5.14. All categories present in variability annexes 1 and 2 (periodic and unsolved variables, respectively) having more than 5 members with the quoted relative distance and colour index precision have been included.

The Hertzsprung-Russell diagram for stars in Part C of the Double and Multiple Systems Annex (i.e. the 'component solutions' of DMSA/C) is shown in Figure 3.5.15. All values have been taken from the main catalogue, so that in the cases where the components are not separated ('*' or '-' in Field H48) the total magnitude has been used, with the consequence that such systems are displaced higher in the diagram compared with single stars. The average value of this offset is expected to be 0.3 mag for components of equal colour index. This is further illustrated in Figure 3.5.16, which shows the ratio of the numbers of double and multiple stars (as in the previous figure) compared with the union of double and multiple stars and the single stars (as in Figure 3.5.6). The distribution is as expected for the ratio of two distributions of which one is slightly offset: for reasonable distributions the maximum ratio is expected near the boundary.

3.5.2. Other Diagrams

Figure 3.5.17 shows the distribution of the relative distance precision σ_π/π as a function of the *Hp* magnitude. The distribution follows rather closely the distribution of *Hp*, as shown in Section 3.2, but somewhat shifted to fainter stars, an effect caused by the fact that the fainter stars tend to lie at larger distances, and consequently have a higher (numerical) value of the precision. Figure 3.5.18 relates the parallax to the *Hp* magnitude for stars with $\sigma_\pi/\pi < 0.2$. The sharp edge at the bottom of the diagram is directly related to this limit, and follows the distribution of σ_π as a function of *Hp*. Nearby stars are found for all magnitudes, but there is a slight increase in concentration for the faintest stars, due to the selection made for the Hipparcos Input Catalogue. Figure 3.5.19 shows the correlation between σ_π/π and π; the main features of this diagram reflect the fact that the parallax standard error is $\sigma_\pi \simeq 1$ mas for most stars in the catalogue. The relationship between the transverse velocity, computed as in Equation 1.2.20, and the parallax is shown in Figure 3.5.20.

Figure 3.5.21 shows the parallax as a function of the $B-V$ colour index, essentially reflecting the features of the histogram of the $B-V$ colour index. The rising feature near $B-V = 1.5$ mag corresponds to the lower part of the main sequence; these intrinsically faint stars could only be observed by Hipparcos if they are relatively nearby.

The relation between the parallax and the total proper motion $|\mu|$ is shown in Figure 3.5.22. The relationship between the total proper motion and the *Hp* magnitude is shown in Figure 3.5.23. For fainter stars there are two groups: the nearby faint stars with high proper motion, and the intrinsically bright, distant stars. The relationship between the total proper motion and the $B-V$ colour index (Figure 3.5.24) follows closely the distribution of stars with this colour index.

The features of the relationship between $Hp-V$ versus $B-V$ (Figure 3.5.25) and between $Hp-V_T$ versus B_T-V_T (Figure 3.5.26) are described in Section 1.3, Appendix 4.

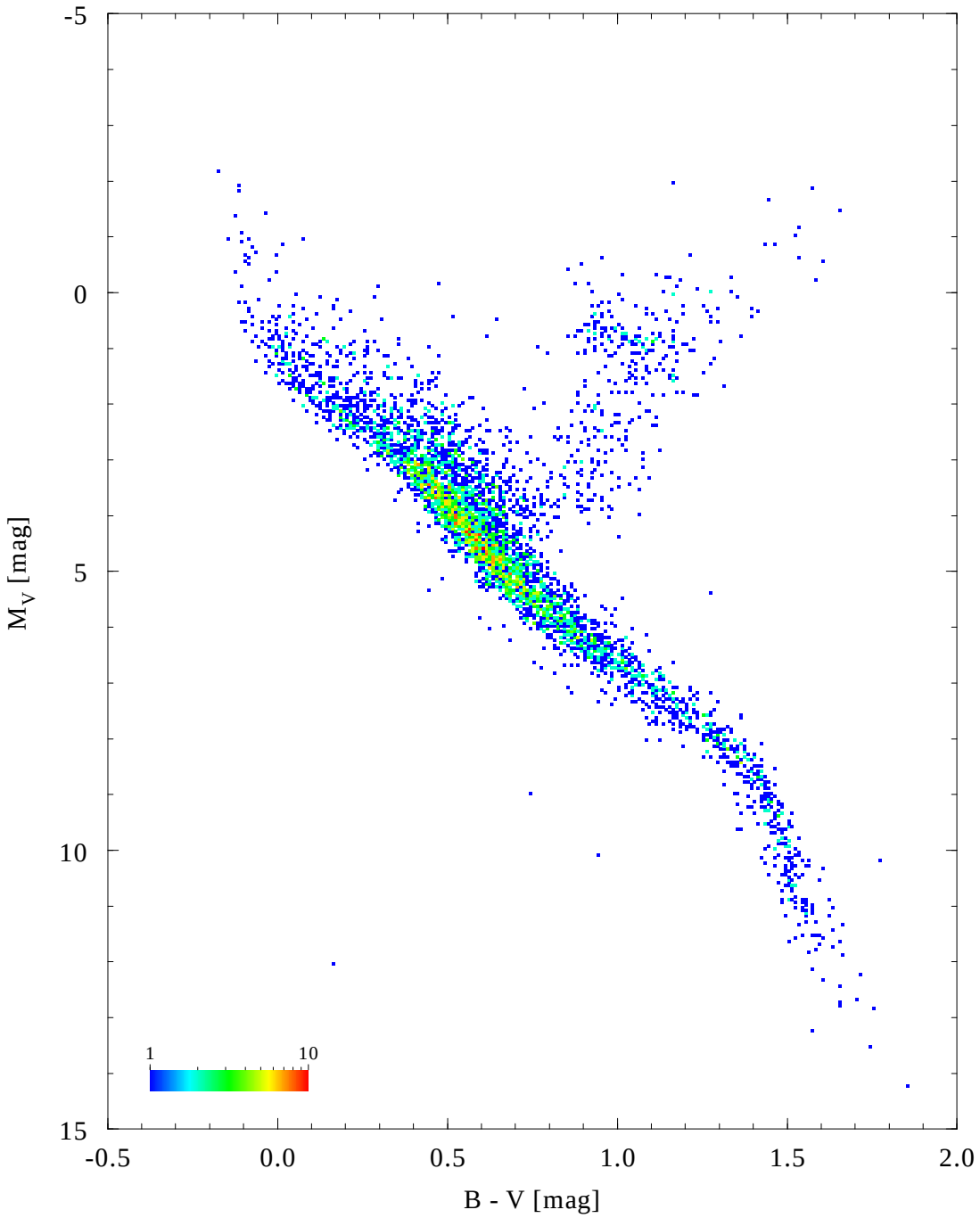

Figure 3.5.1. *$(M_V, B-V)$ diagram for the 4902 single stars from the Hipparcos Catalogue with relative distance precision $\sigma_\pi/\pi < 0.05$ and $\sigma_{B-V} \leq 0.025$ mag. Colours indicate number of stars in a cell of 0.01 mag in $B-V$ and 0.05 mag in M_V.*

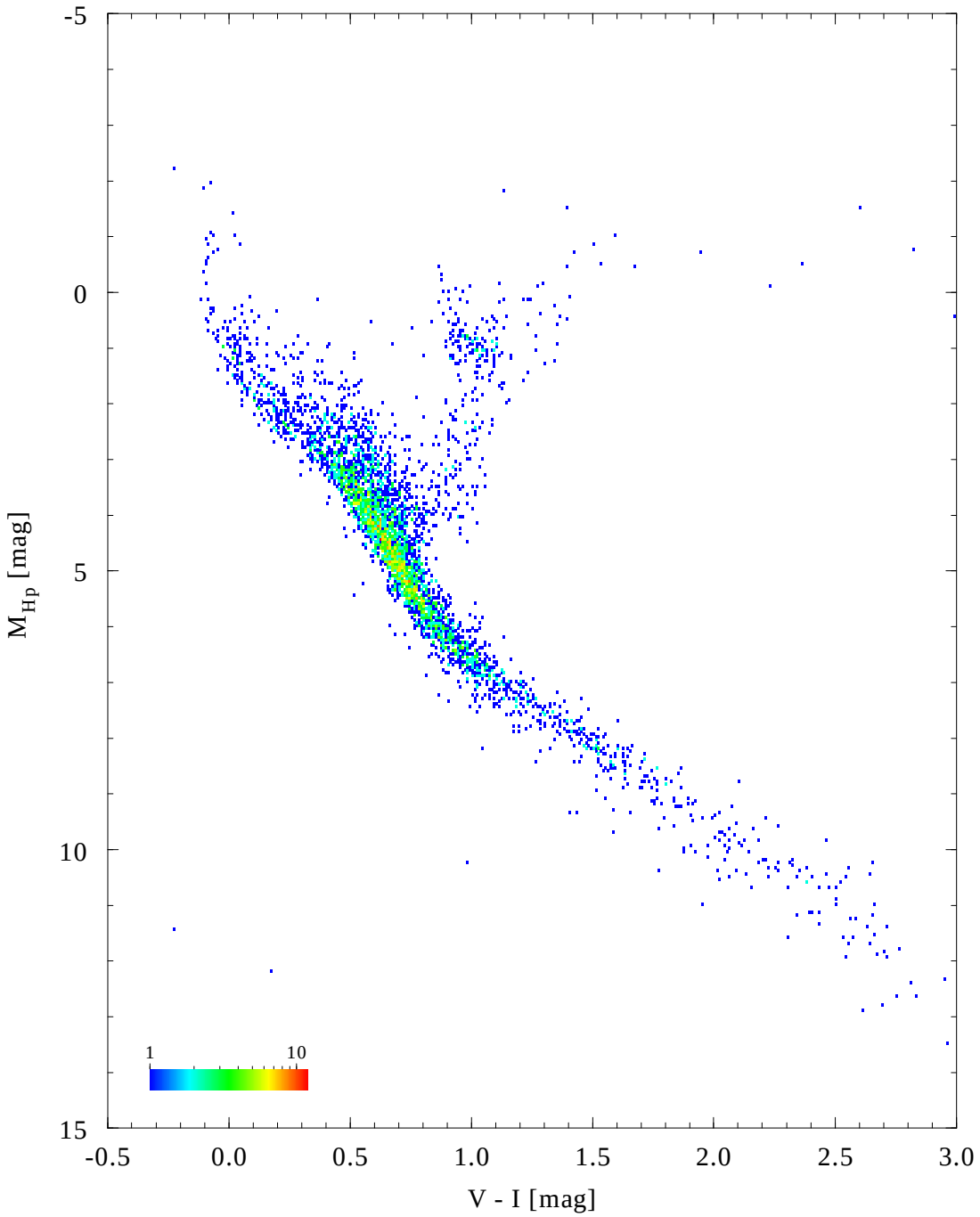

Figure 3.5.2. *$(M_{Hp}, V-I)$ diagram for the 4477 single stars from the Hipparcos Catalogue with relative distance precision $\sigma_\pi/\pi < 0.05$ and $\sigma_{V-I} \leq 0.025$ mag. Colours indicate number of stars in a cell of 0.01 mag in $V-I$ and 0.05 mag in M_{Hp}.*

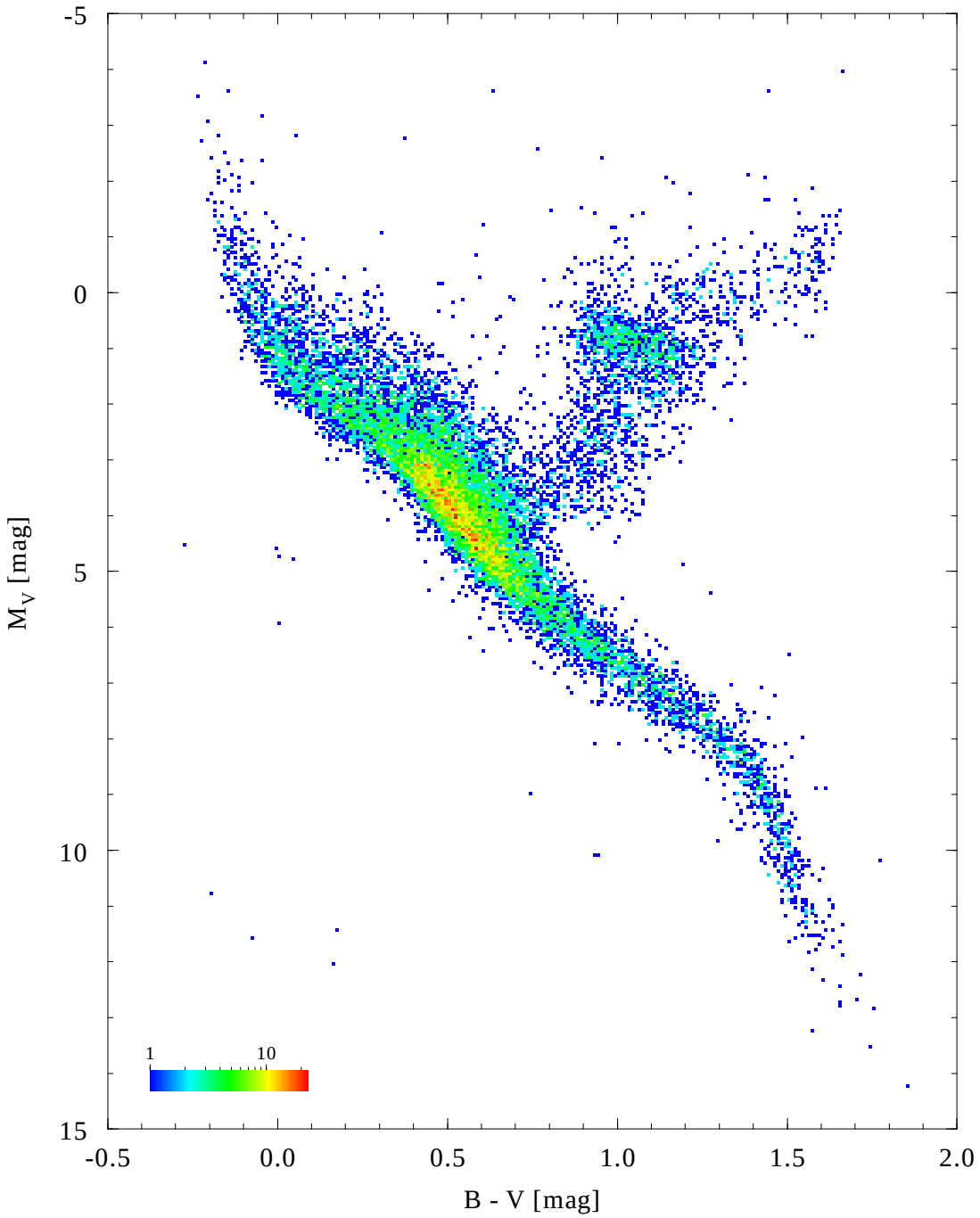

Figure 3.5.3. *$(M_V, B-V)$ diagram for the 16 631 single stars from the Hipparcos Catalogue with relative distance precision $\sigma_\pi/\pi < 0.1$ and $\sigma_{B-V} \leq 0.025$ mag. Colours indicate number of stars in a cell of 0.01 mag in $B-V$ and 0.05 mag in M_V.*

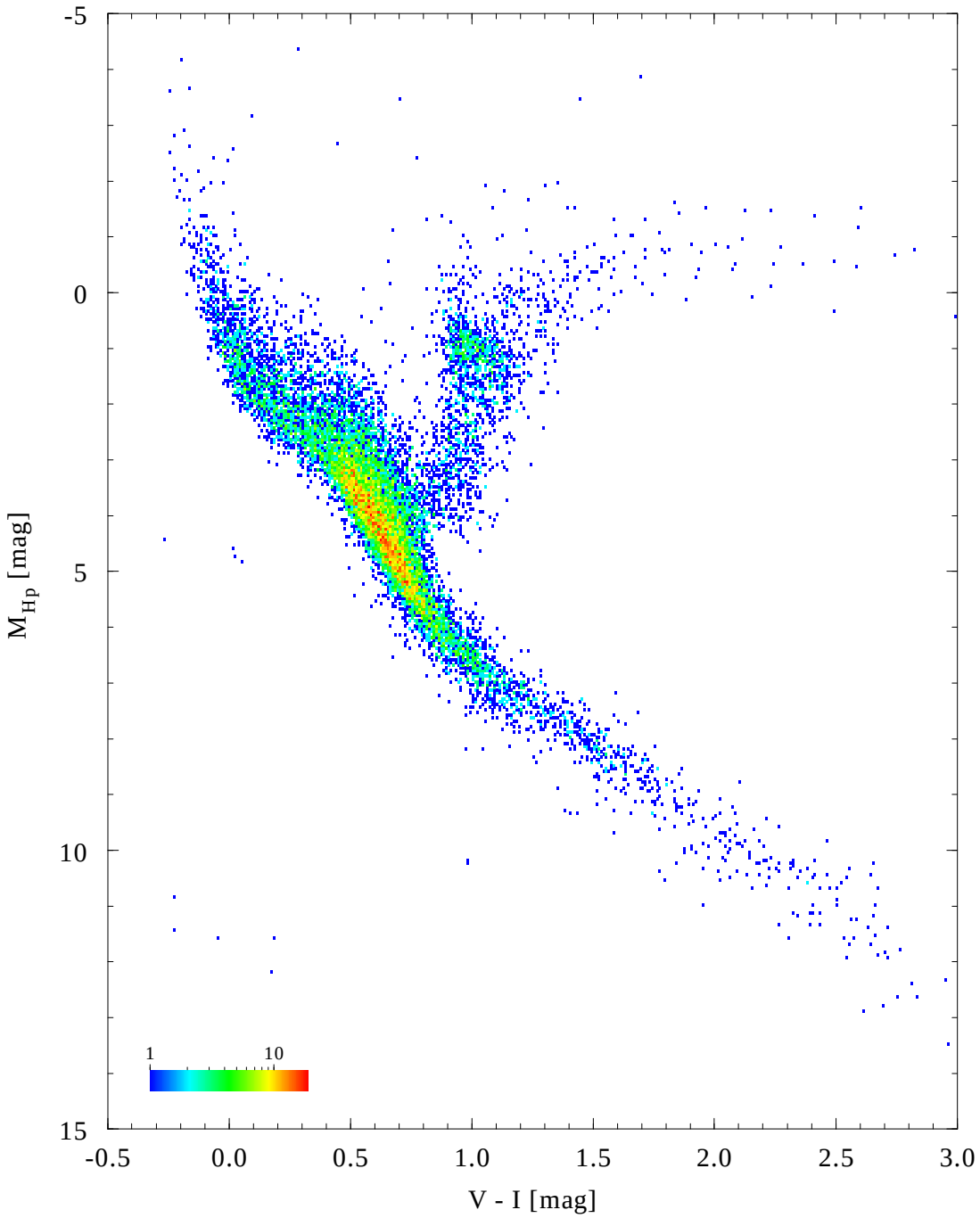

Figure 3.5.4. *$(M_{Hp}, V-I)$ diagram for the 15 727 single stars from the Hipparcos Catalogue with relative distance precision $\sigma_\pi/\pi < 0.1$ and $\sigma_{V-I} \leq 0.025$ mag. Colours indicate number of stars in a cell of 0.01 mag in $V-I$ and 0.05 mag in M_{Hp}.*

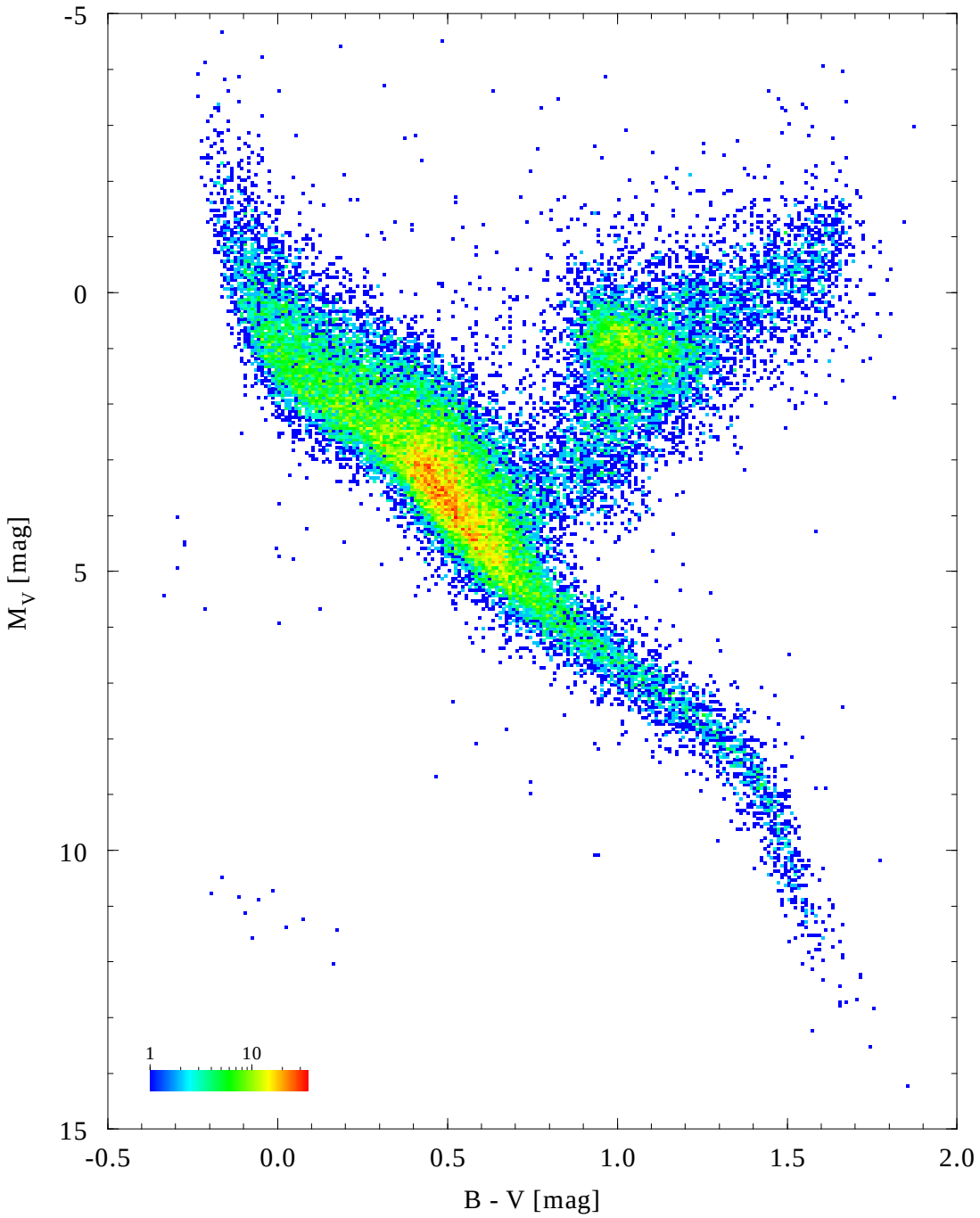

Figure 3.5.5. *$(M_V, B-V)$ diagram for the 41 704 single stars from the Hipparcos Catalogue with relative distance precision $\sigma_\pi/\pi < 0.2$ and $\sigma_{B-V} \leq 0.05$ mag. Colours indicate number of stars in a cell of 0.01 mag in $B-V$ and 0.05 mag in M_V.*

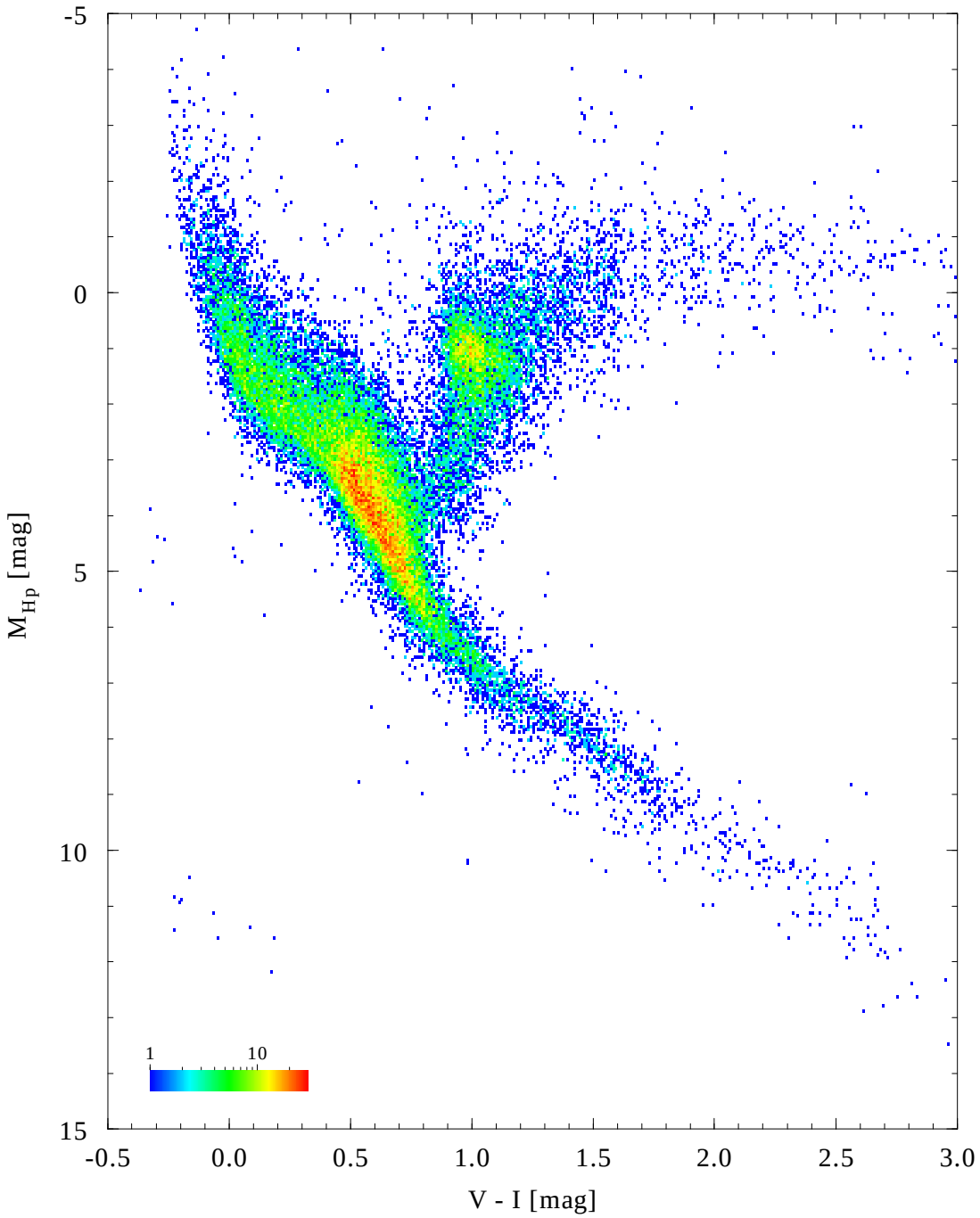

Figure 3.5.6. *$(M_{Hp}, V-I)$ diagram for the 41 453 single stars from the Hipparcos Catalogue with relative distance precision $\sigma_\pi/\pi < 0.2$ and $\sigma_{V-I} \leq 0.05$ mag. Colours indicate number of stars in a cell of 0.01 mag in $V-I$ and 0.05 mag in M_{Hp}.*

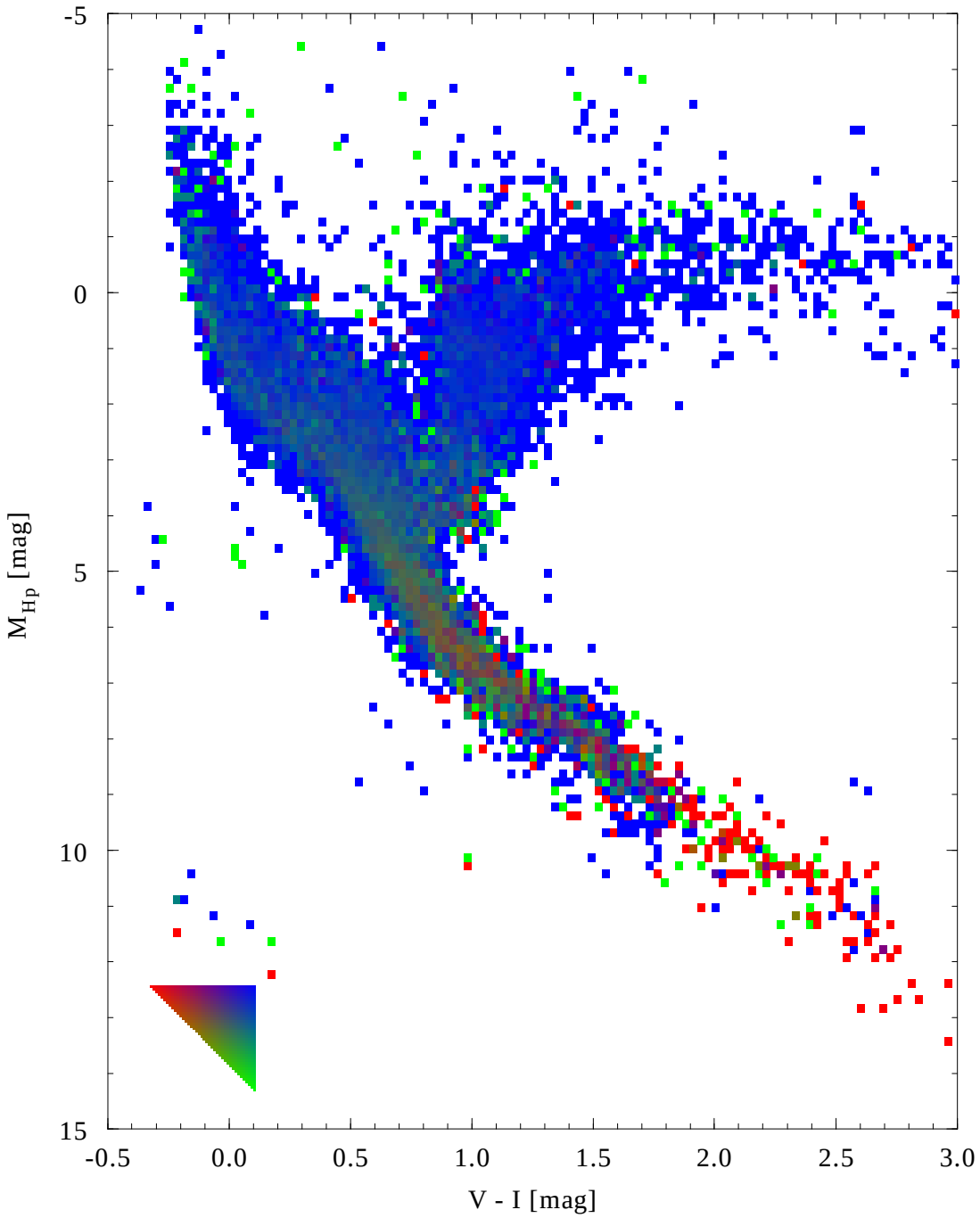

Figure 3.5.7. *Relative contribution of single stars with relative distance precision $\sigma_\pi/\pi < 0.05$ (red), $0.05 \leq \sigma_\pi/\pi < 0.1$ (green), and $0.1 \leq \sigma_\pi/\pi < 0.2$ (blue) to the $(M_{Hp}, V-I)$ diagram. The cell size is 0.03 mag in $V-I$ and 0.15 mag in M_{Hp}. The triangular colour scale covers all possibilities (the contribution from the 'red' category decreases from 100 per cent to 0 per cent from left to right, the contribution from the 'green' category decreases from 100 per cent to 0 per cent from bottom to top, and the 'blue' category comprises the remaining stars, and is therefore 100 per cent at top right).*

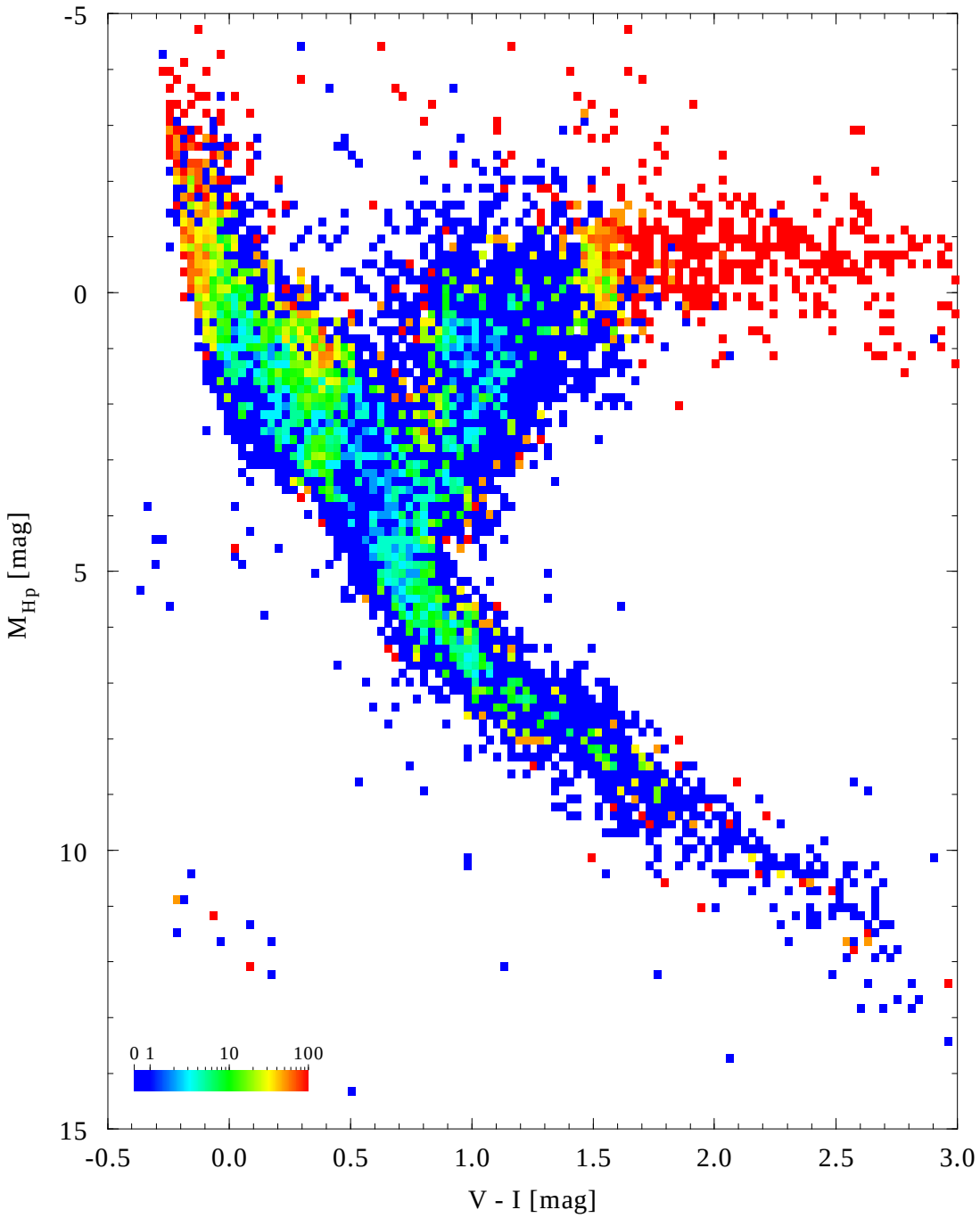

Figure 3.5.8. *Fraction of stars that are variable (Field H6 non-blank) in a $(M_{Hp}, V-I)$ diagram. In each cell of 0.03 mag in $V-I$ and 0.15 mag in M_{Hp}, the percentage of variable stars is coded according to the colour scale.*

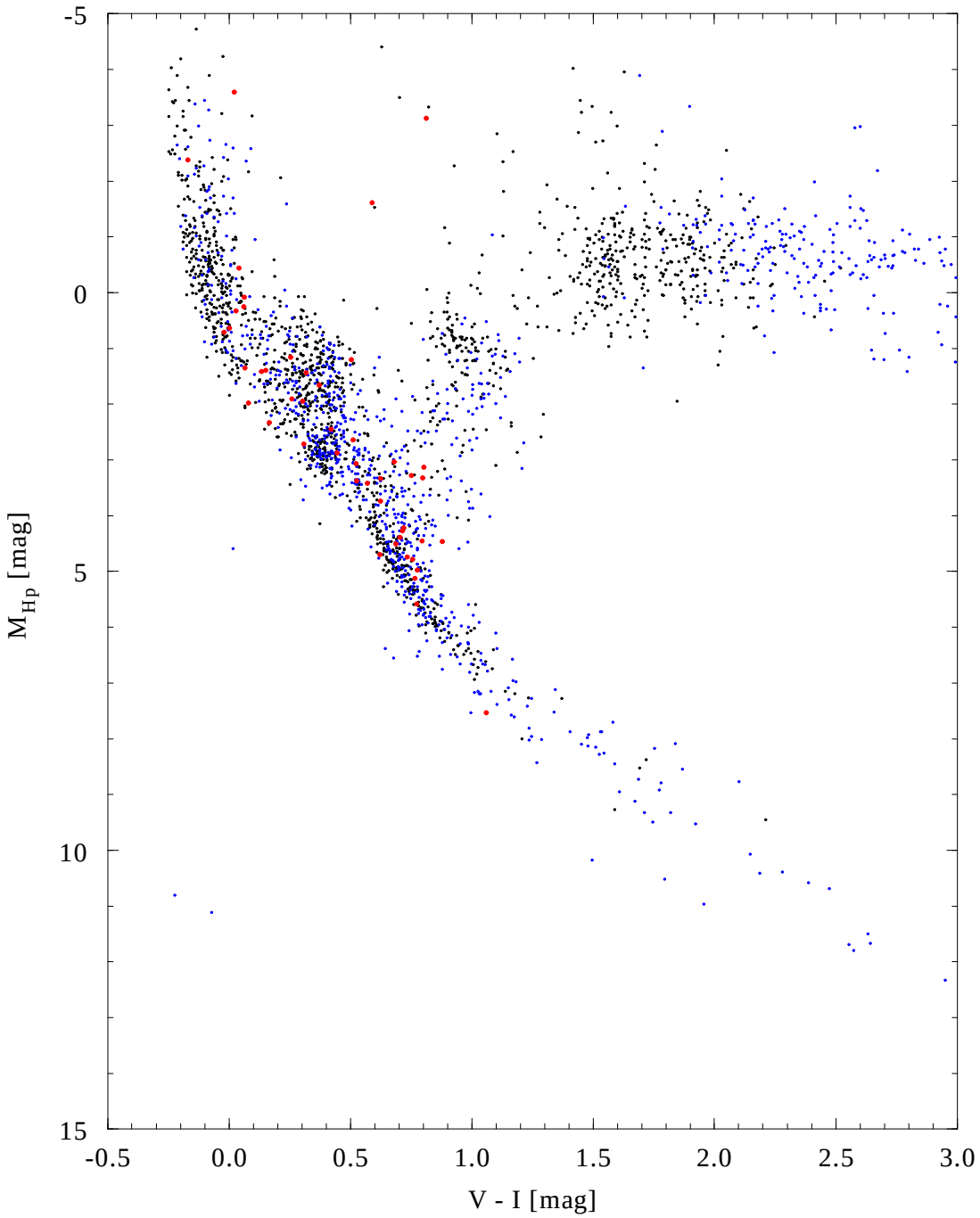

Figure 3.5.9. *($M_{Hp}, V-I$) diagram for single stars from the Hipparcos Catalogue with coarse variability indicator (Field H6) non-blank, and with relative distance precision $\sigma_\pi/\pi < 0.2$ and $\sigma_{V-I} \leq 0.05$. The values of the coarse variability flag are coded by different colours: 1 (< 0.06 mag, 1512 stars) = black, 2 (0.06 – 0.6 mag, 977 stars) = blue, and 3 (> 0.6 mag, 48 stars) = red.*

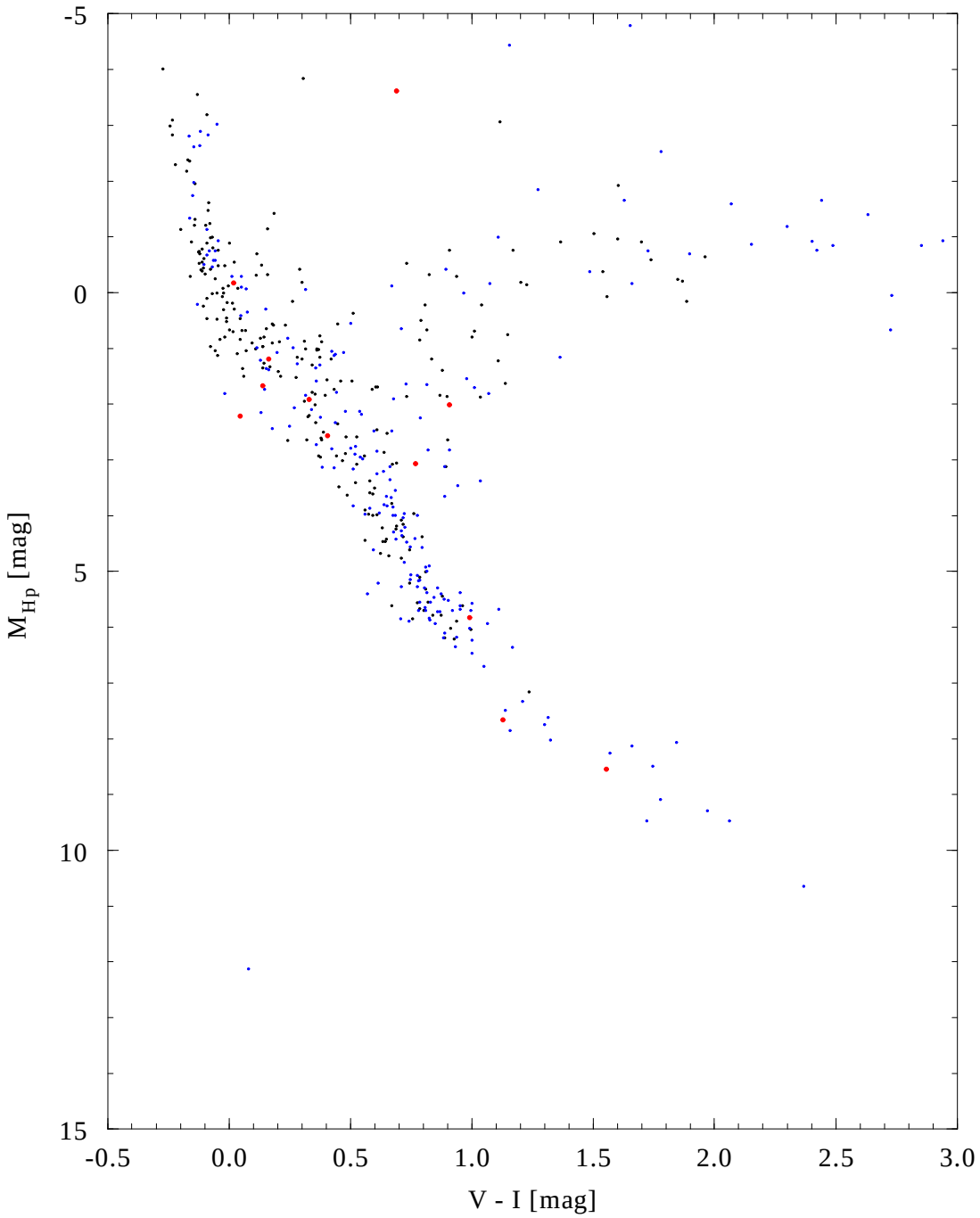

Figure 3.5.10. *$(M_{Hp}, V-I)$ diagram for stars from all parts of the DMSA with coarse variability indicator (Field H6) non-blank, and with relative distance precision $\sigma_\pi/\pi < 0.2$ and $\sigma_{V-I} \leq 0.05$. The values of the coarse variability flag are coded by different colours: 1 (< 0.06 mag, 238 stars) = black, 2 (0.06 – 0.6 mag, 206 stars) = blue, and 3 (> 0.6 mag, 16 stars) = red.*

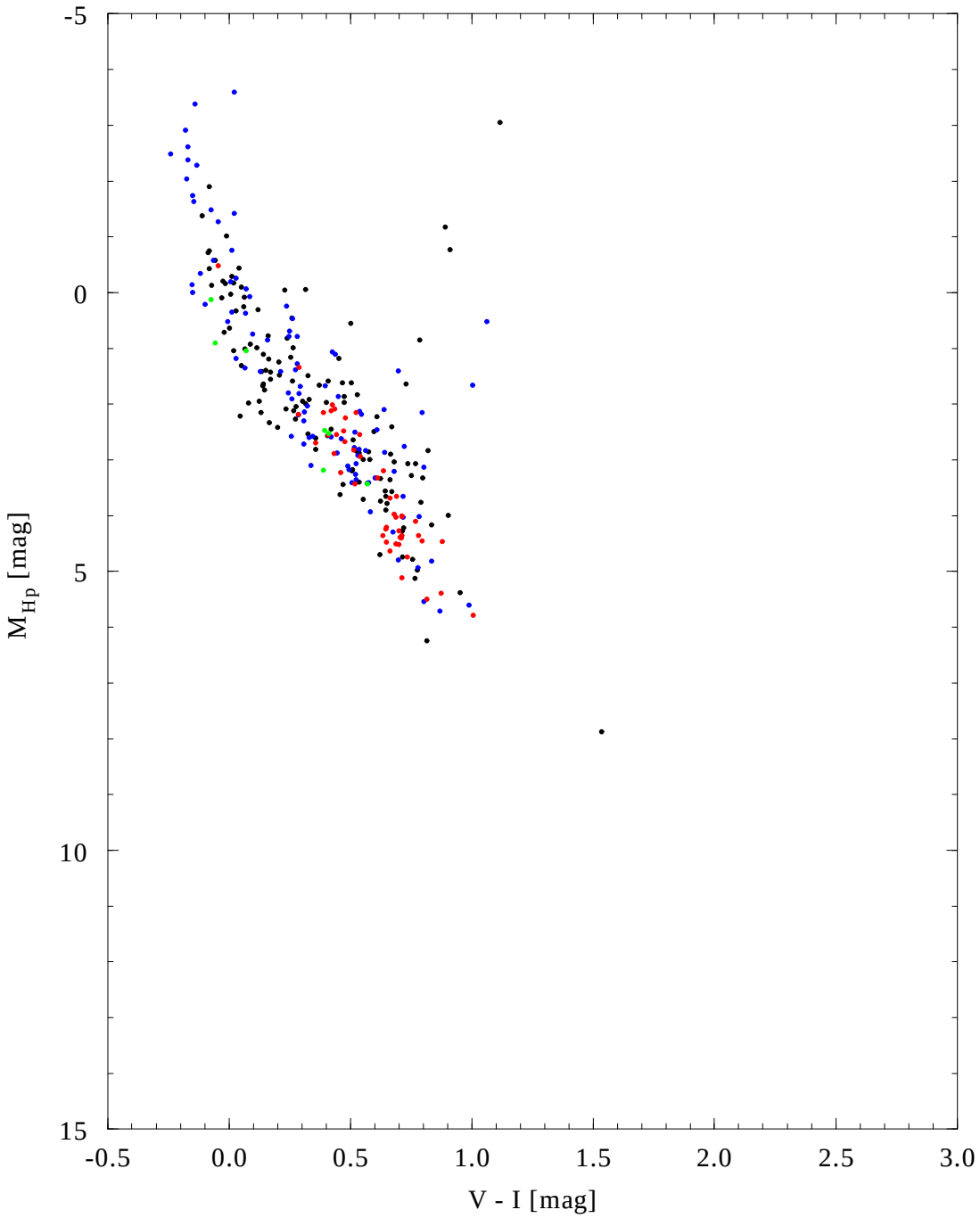

Figure 3.5.11. *($M_{Hp}, V-I$) diagram for eclipsing binary stars in the Variability Annex, Part 1 (Periodic Variables) with relative distance precision $\sigma_\pi/\pi < 0.2$ and $\sigma_{V-I} \leq 0.05$ mag. ●: Algol type (EA, 125 stars), ●: β Lyrae type (EB, 95 stars), ●: W Ursae Majoris type (EW, 48 stars), ●: other E (7 stars).*

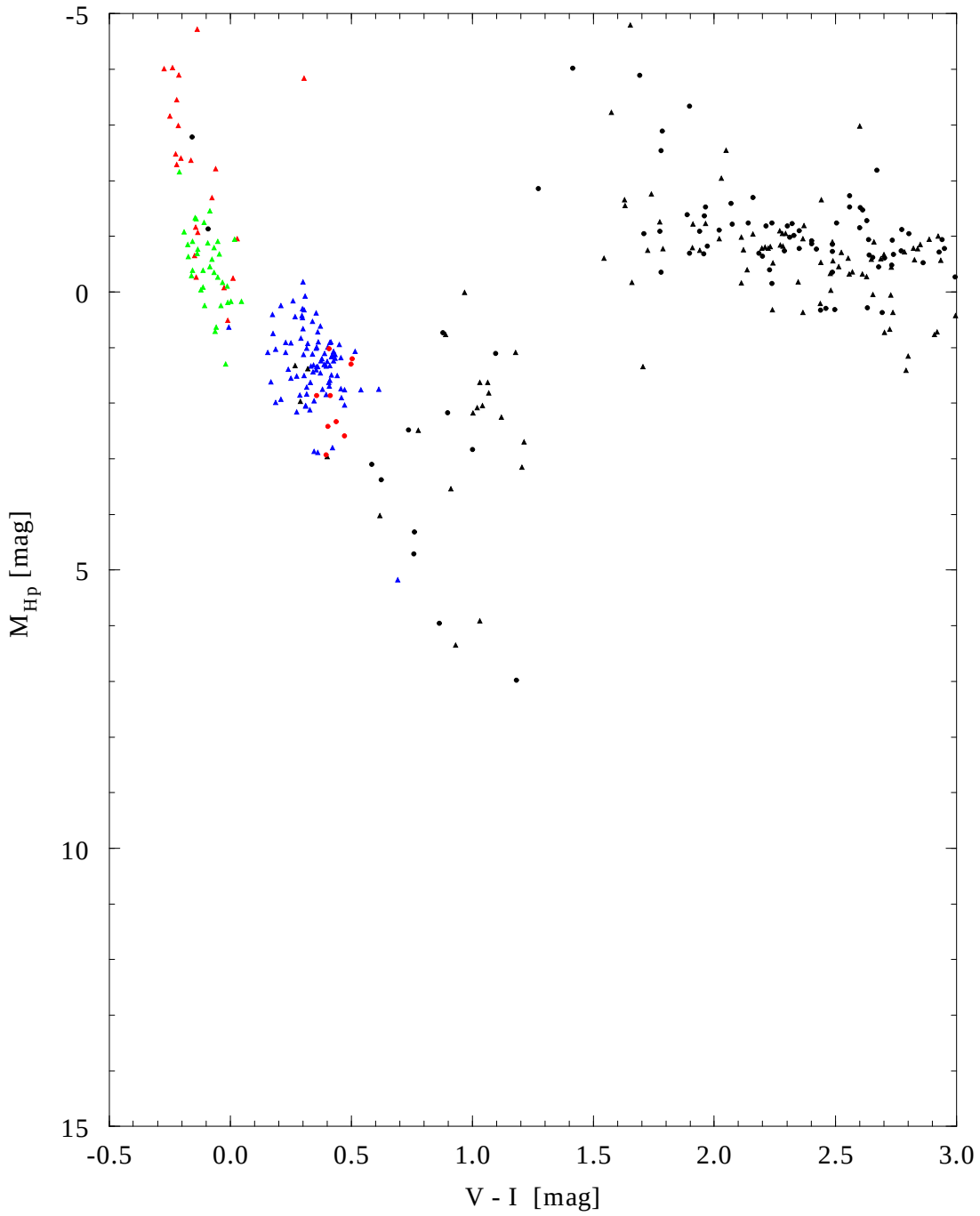

Figure 3.5.12. *(M_{Hp}, $V-I$) diagram for pulsating types of variable stars in the Variability Annexes, Part 1 (Periodic Variables) and Part 2 (Unsolved Variables) with relative distance precision $\sigma_\pi/\pi < 0.2$ and $\sigma_{V-I} \leq 0.05$ mag. ▲: semi-regular (SR..., 116 stars), ▲: δ Scuti type (DSCT, 89 stars), ▲: β Cephei type (BCEP..., 24 stars), ▲: small-amplitude multi-period pulsating stars (SPB, 35 stars), ●: slow irregular (L..., 93 stars), ●: RR Lyrae type (RR..., 9 stars).*

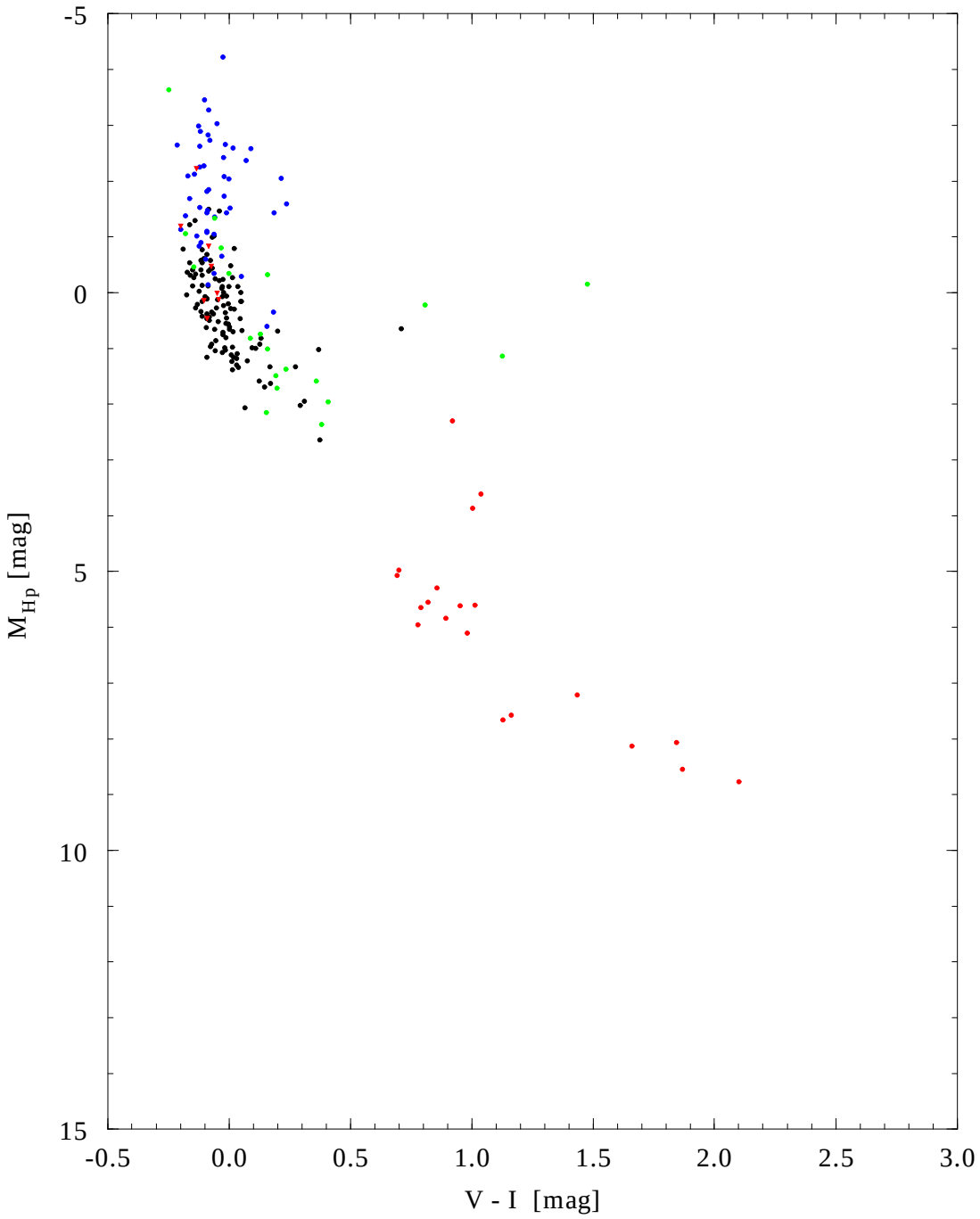

Figure 3.5.13. *($M_{Hp}, V-I$) diagram for rotating types of variable stars in the Variability Annexes, Part 1 (Periodic Variables) and Part 2 (Unsolved Variables) with relative distance precision $\sigma_\pi/\pi < 0.2$ and $\sigma_{V-I} \leq 0.05$ mag. ●: α^2 Canum Venaticorum type (ACV, 114 stars), ●: γ Cassiopeiae type (GCAS, 49), ●: BY Draconis type (BY, 20 stars), ●: rotating ellipsoidal type (ELL..., 20 stars), ▼: SX Arietis type (SXARI, 8 stars).*

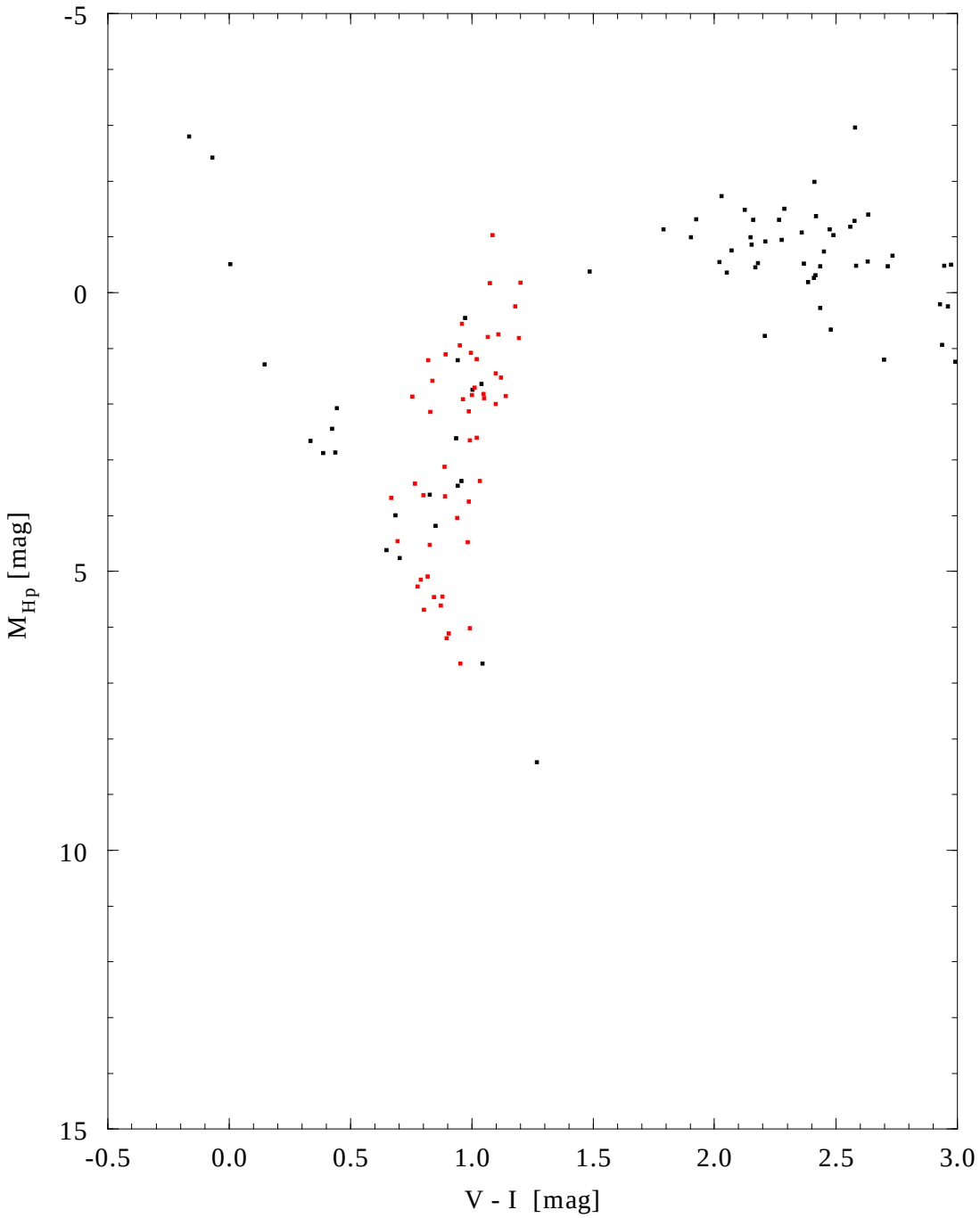

Figure 3.5.14. *$(M_{Hp}, V-I)$ diagram for eruptive types of variable stars in the Variability Annexes, Part 1 (Periodic Variables) and Part 2 (Unsolved Variables) with relative distance precision $\sigma_\pi/\pi < 0.2$ and $\sigma_{V-I} \leq 0.05$. ■: irregular (I..., 76 stars), ■: RS Canum Venaticorum type (RS, 50 stars).*

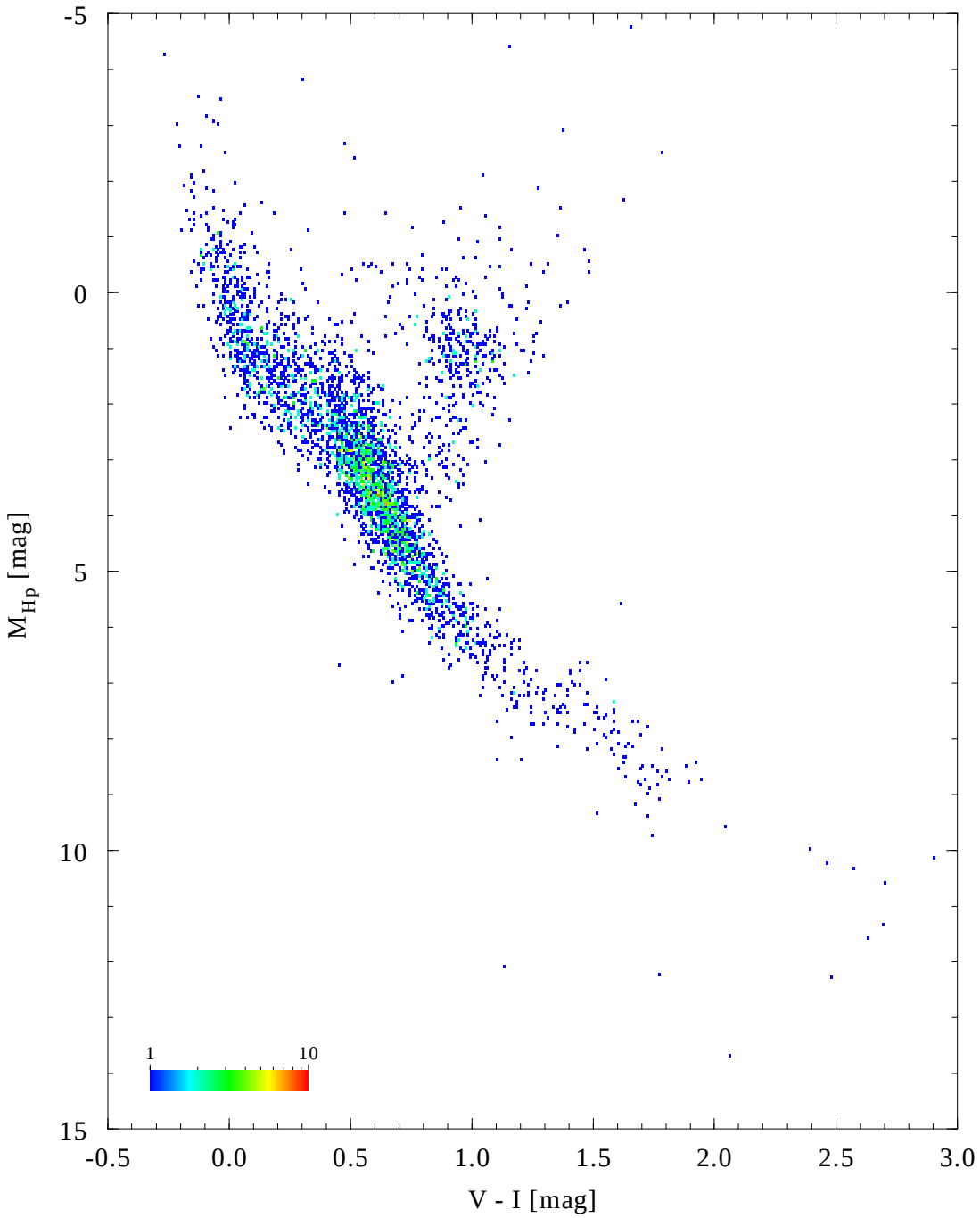

Figure 3.5.15. *$(M_{Hp}, V-I)$ diagram for 3926 stars in the Double and Multiple Systems Annex, Component Solutions (DMSA/C) with relative distance precision $\sigma_\pi/\pi < 0.2$ and $\sigma_{V-I} \leq 0.05$ mag. All parameters are taken from the main Hipparcos Catalogue. Colours indicate the number of stars in a cell of 0.01 mag in $V-I$ and 0.05 mag in M_{Hp}.*

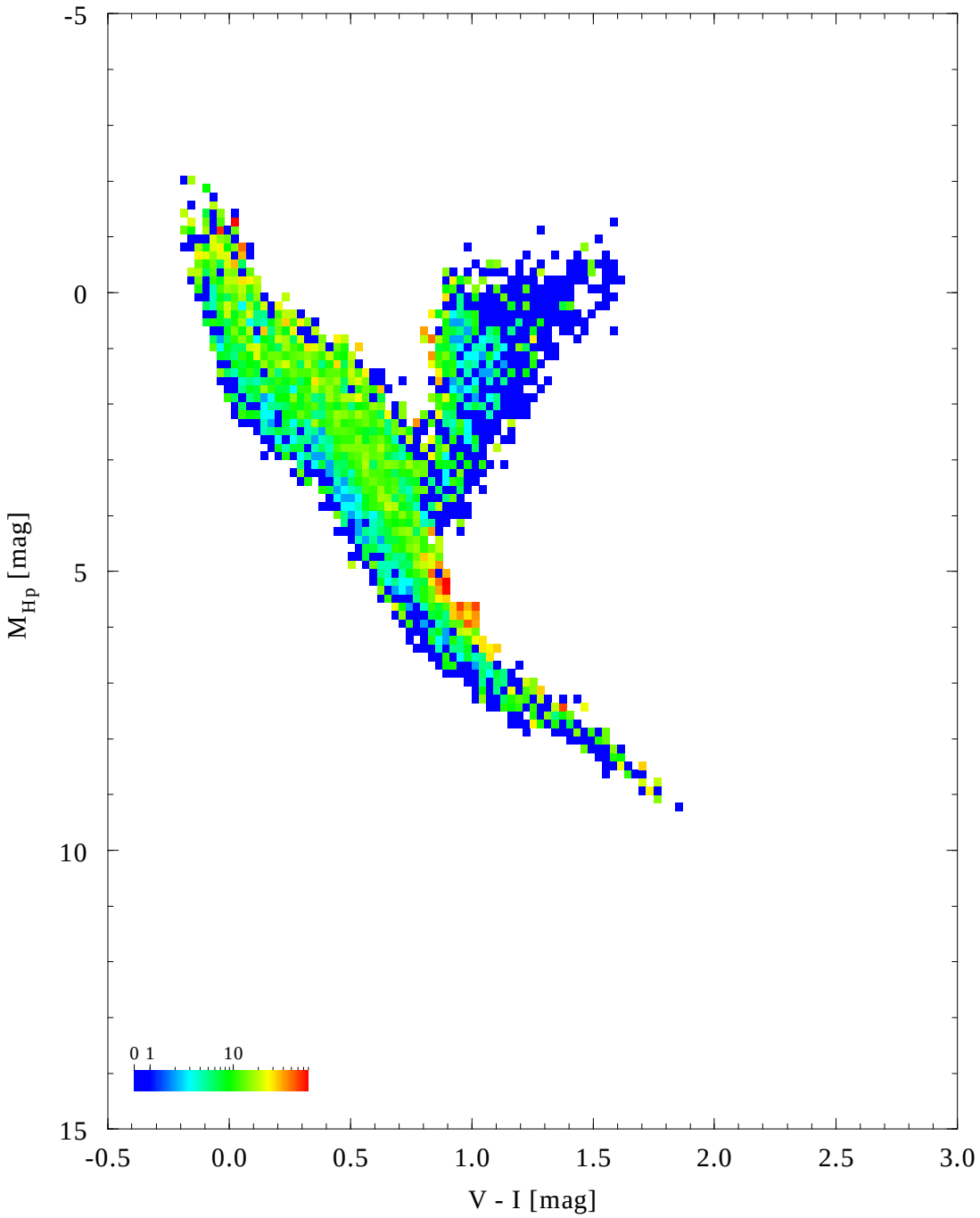

Figure 3.5.16. *Fraction of stars that are double or multiple (Field H59 = 'C') in the $(M_{Hp}, V-I)$ diagram. In each cell of 0.03 mag in $V-I$ and 0.15 mag in M_{Hp} with at least 5 stars, the relevant percentage is coded according to the colour scale.*

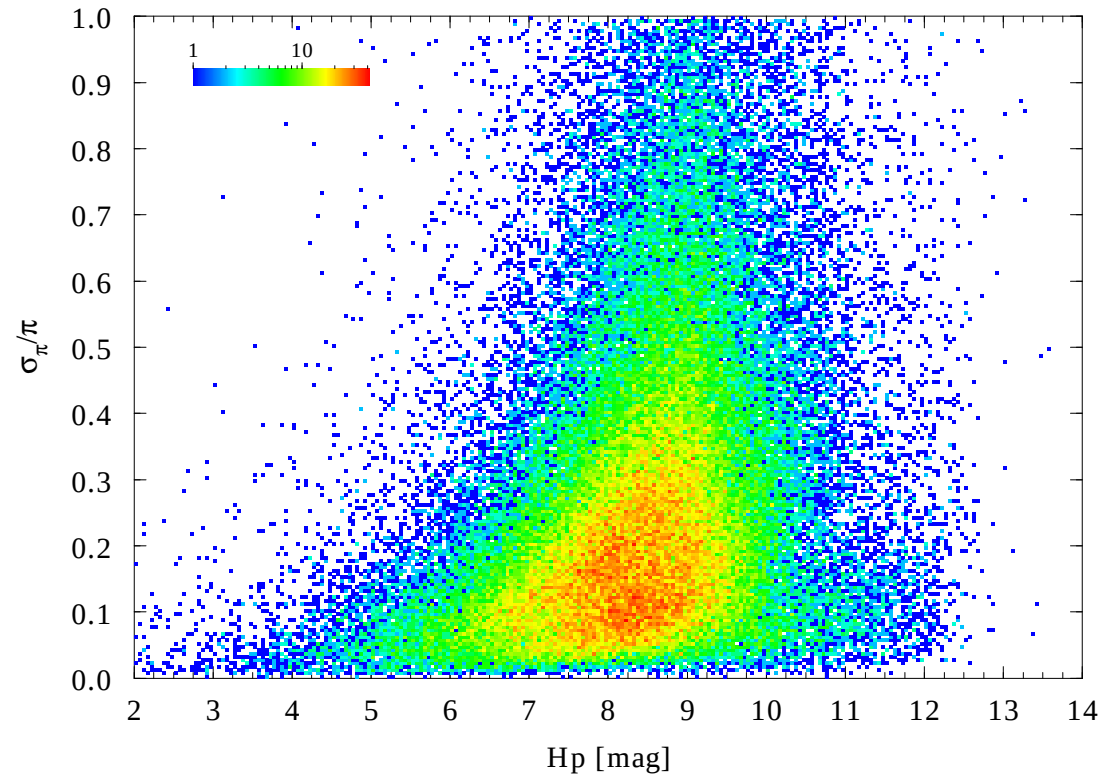

Figure 3.5.17. *Hipparcos Catalogue: relative distance precision σ_π/π versus Hp magnitude (bin size 0.05 mag in Hp and 0.005 in σ_π/π).*

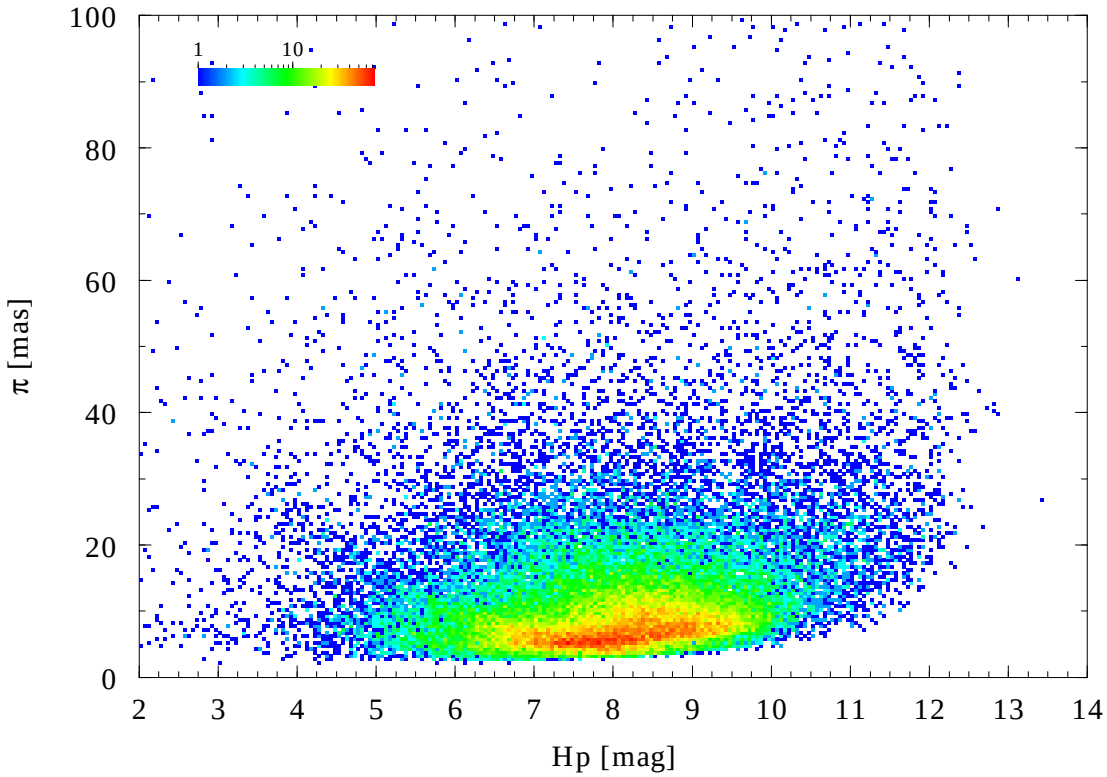

Figure 3.5.18. *Hipparcos Catalogue: parallax π versus Hp magnitude for all objects with $\sigma_\pi/\pi \leq 0.2$ (bin size 0.05 mag in Hp and 0.5 mas in π).*

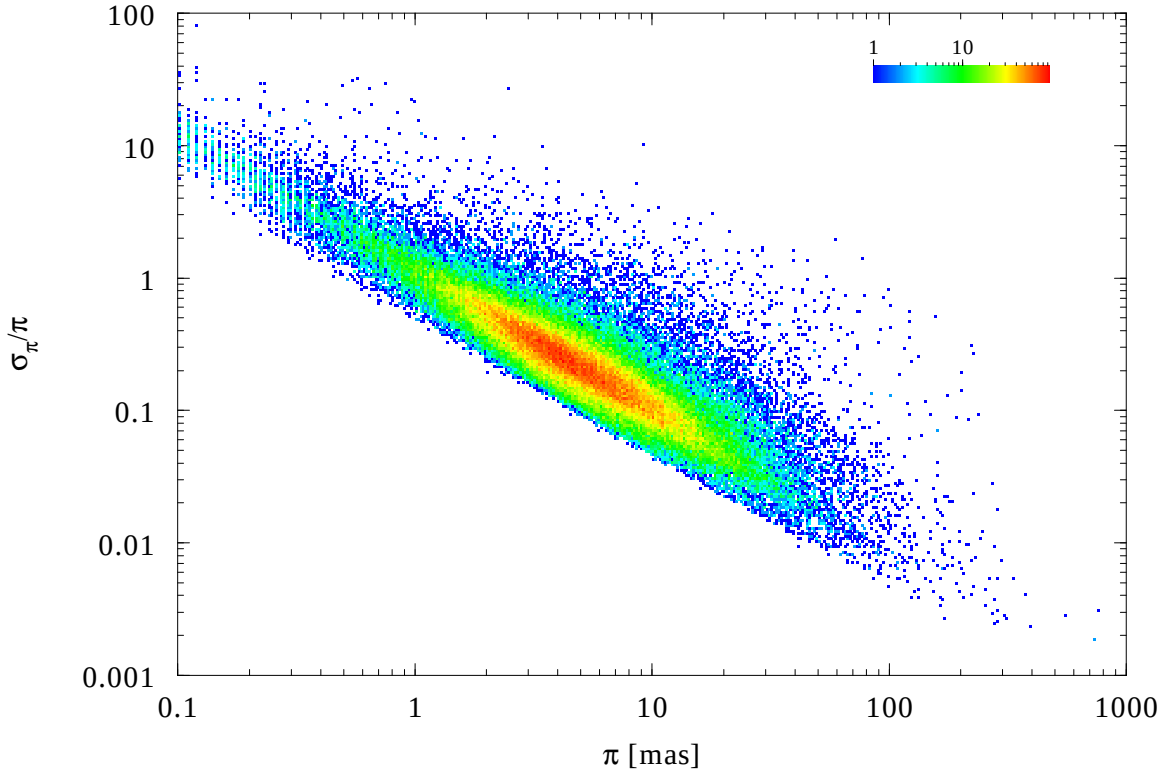

Figure 3.5.19. *Hipparcos Catalogue: relative distance precision σ_π/π versus parallax π (bin size 0.01 dex in π and 0.02 dex in σ_π/π).*

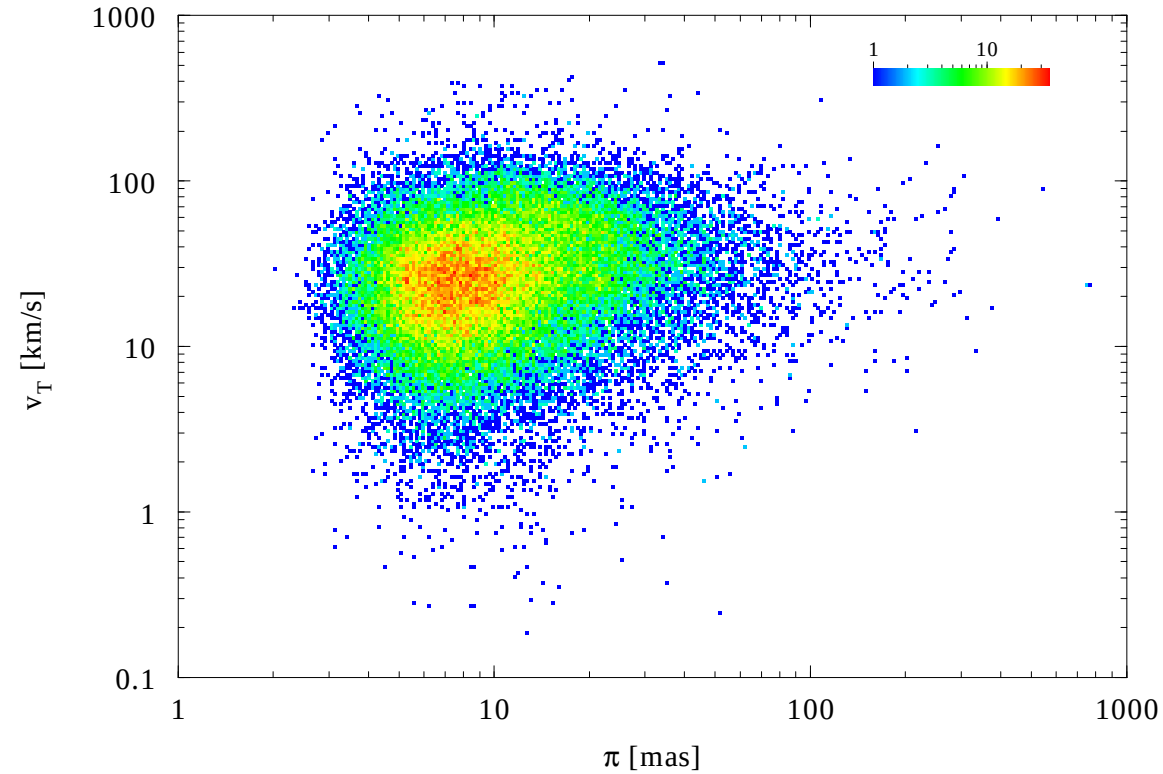

Figure 3.5.20. *Hipparcos Catalogue: tranverse velocity v_T versus parallax π (bin size 0.01 dex in π and 0.02 dex in v_T).*

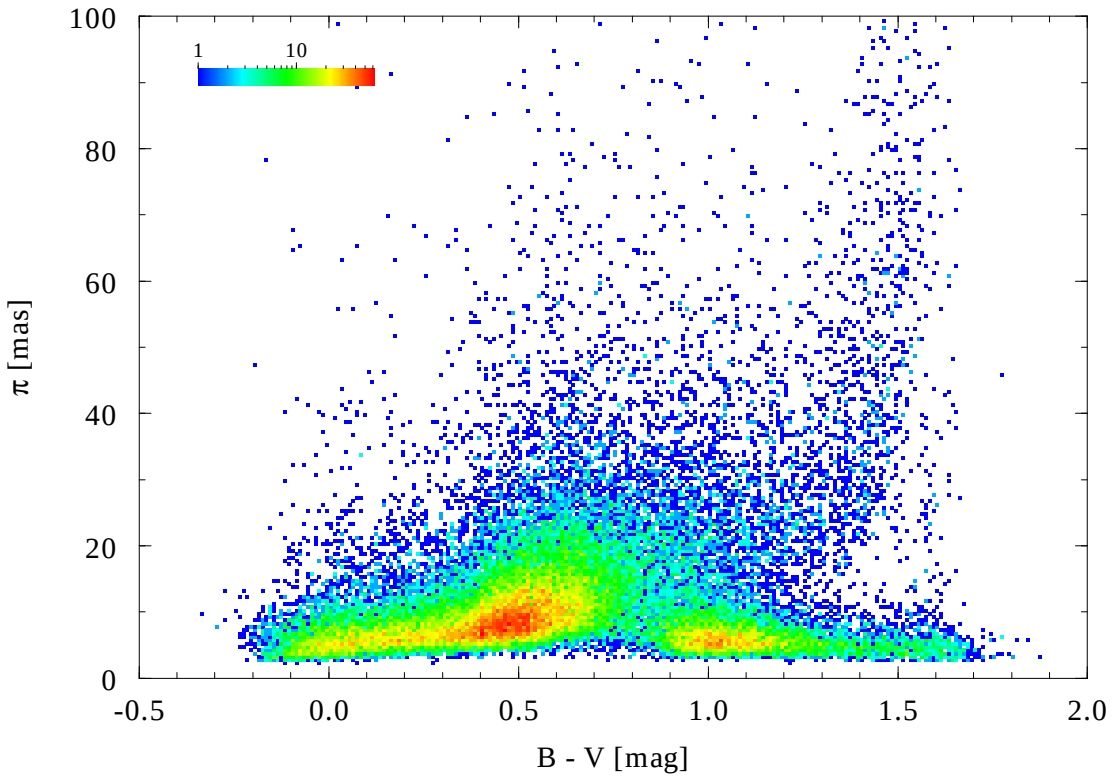

Figure 3.5.21. *Hipparcos Catalogue: parallax π versus $B-V$ colour index for all objects with $\sigma_\pi/\pi \leq 0.2$ and $\sigma_{B-V} \leq 0.1$ (bin size 0.01 mag in $B-V$ and 0.5 mas in π).*

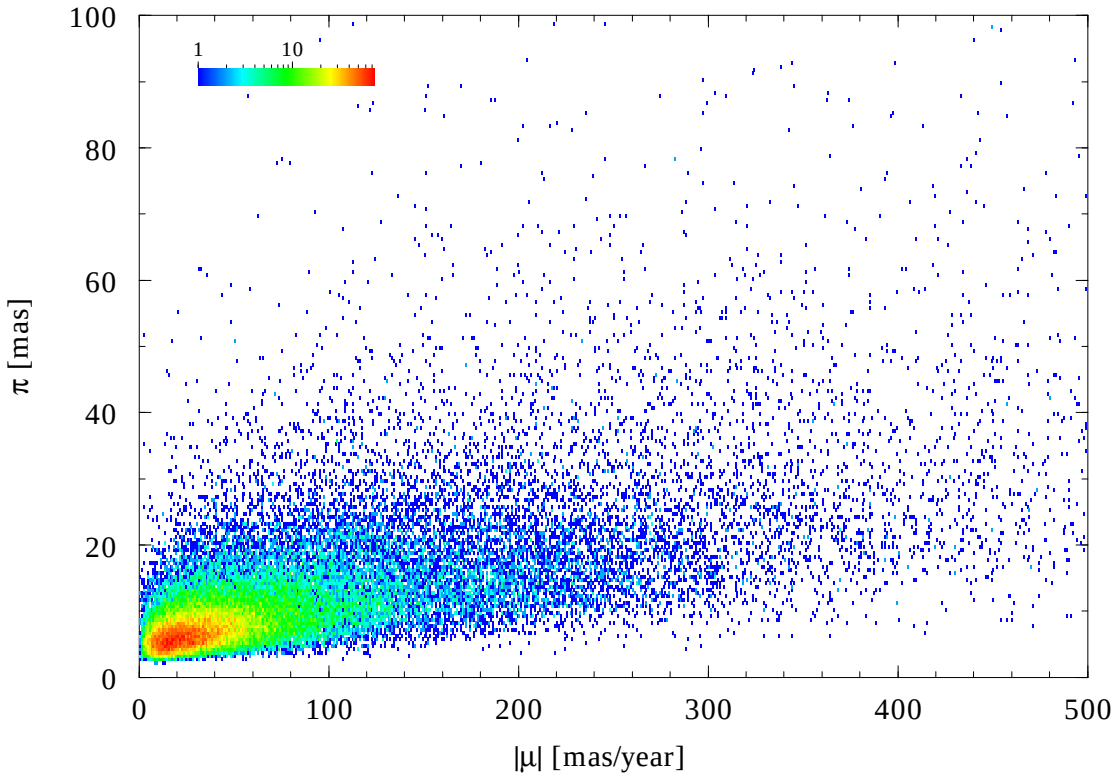

Figure 3.5.22. *Hipparcos Catalogue: parallax π versus total proper motion $|\boldsymbol{\mu}|$ for all objects with $\sigma_\pi/\pi \leq 0.2$ (bin size 1 mas/year in $|\boldsymbol{\mu}|$ and 0.5 mas in π).*

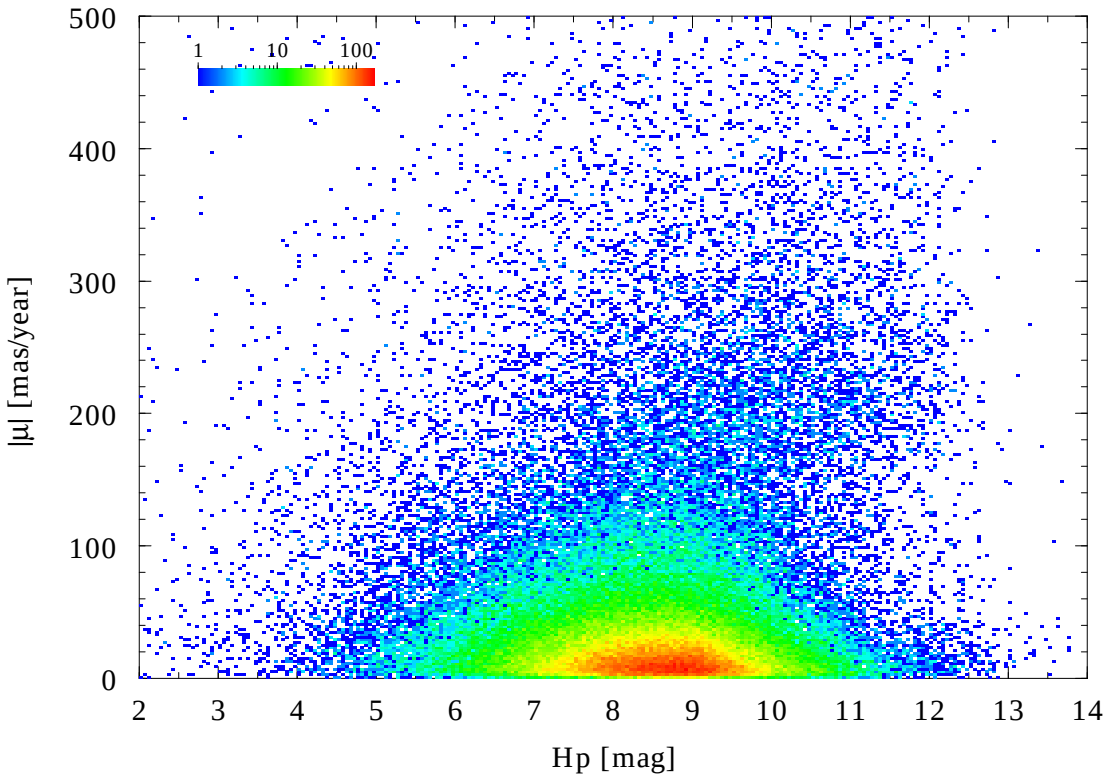

Figure 3.5.23. *Hipparcos Catalogue: total proper motion $|\boldsymbol{\mu}|$ versus Hp magnitude (bin size 0.05 mag in Hp and 2 mas/year in $|\boldsymbol{\mu}|$).*

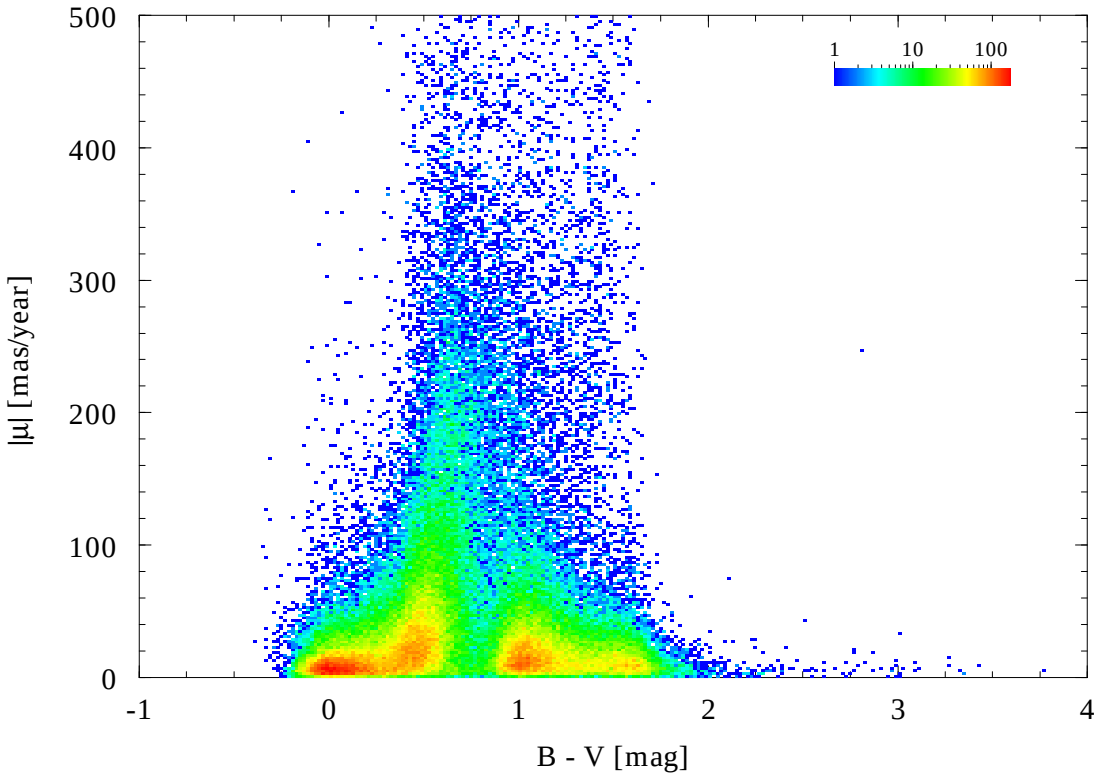

Figure 3.5.24. *Hipparcos Catalogue: total proper motion $|\boldsymbol{\mu}|$ versus $B-V$ colour index for all objects with $\sigma_{B-V} \leq 0.1$ mag (bin size 0.02 mag in $B-V$ and 2 mas/year in $|\boldsymbol{\mu}|$).*

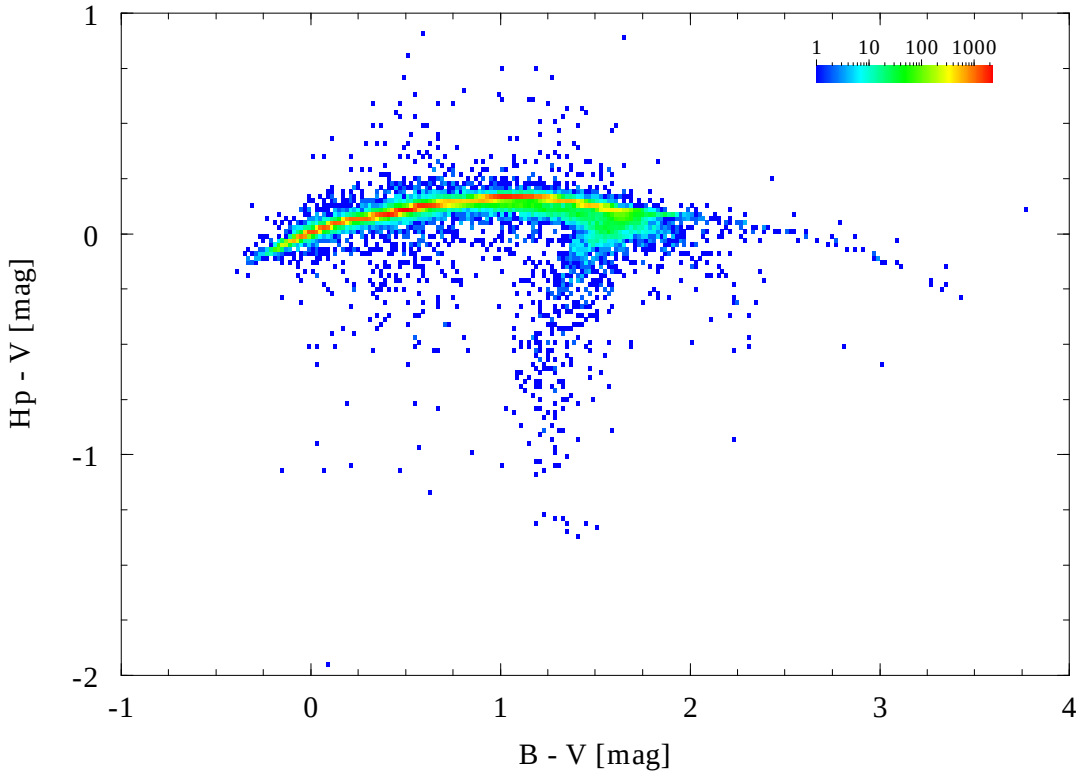

Figure 3.5.25. *Hipparcos Catalogue: $Hp - V$ versus $B - V$ colour index for all objects with $\sigma_{B-V} \leq 0.1$ mag (bin size 0.02 mag in both axes).*

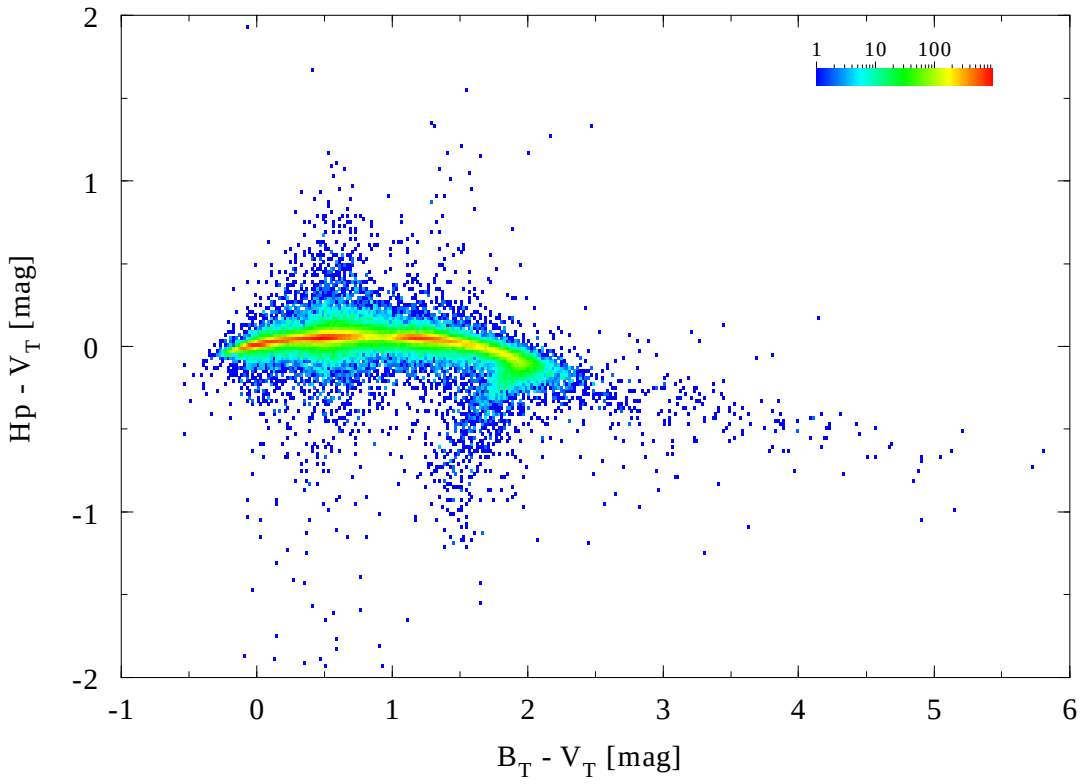

Figure 3.5.26. *Hipparcos Catalogue: $Hp - V_T$ versus $B_T - V_T$ colour index (bin size 0.02 mag in both axes).*